

Stopping Power of Some Pure Metals for 25–250-keV Hydrogen Ions*

A. Valenzuela,† W. Meckbach, A. J. Kestelman, and J. C. Eckardt‡
Centro Atómico Bariloche and Instituto de Física "Dr. J. A. Balseiro,"
San Carlos de Bariloche, Rio Negro, Argentina

(Received 20 July 1971; revised manuscript received 19 January 1972)

Electronic stopping powers for a hydrogen beam at energies between 25 and 250 keV are measured in the metals Ni, Cu, Ag, Sn, and Au using the straightforward technique of measuring the energy loss of a beam traversing a thin target foil. The metal foils, fabricated specifically for this purpose, are self-supported and thin enough to ensure an energy loss of 10% or less for a 25-keV proton beam. The measured stopping powers are given relative to accepted published values at 250 keV. The results are compared to those of other authors, primarily at the low-energy end of the present measurements where a comparison with the theory of Lindhard and Scharff is also possible. Available information about stopping powers of hydrogen beams in other elements together with the present results are represented as a function of z_2 , the atomic number of the target material. A periodic structure in this diagram is observed which can be related to the filling of electronic shells in the target atoms.

I. INTRODUCTION

Stopping-power curves for hydrogen beams in metallic targets as presented by Whaling¹ are generally accepted as being reliable. These data were brought up to date by Demirlioglu and Whaling.² At energies higher than 1 MeV, the curves are constructed by fitting the experimental data to the theory of Livingston and Bethe³ including Bloch's⁴ criterion.

At energies down to 400 keV, where charge-changing collisions play an increasingly important role in the stopping process, the curves reported by Whaling are an interpolation of experimental results from several authors.

In what follows we restrict the discussion to the target materials used in our work.

Whaling reports the measurements of Bader *et al.*⁵ which cover the energy range down to 50 keV in Cu and Au, and down to 200 keV in Ni. Values which deviate considerably from the experimental average are not used in the evaluation of Whaling. Amongst these are the data reviewed by Allison and Warshaw⁶ for the target materials Cu, Ag, and Au.

Later measurements of Porat and Ramavataram⁷ start at 200 keV and are in good agreement with Whaling's curve above 400 keV. Recently, White and Mueller⁸ measured the stopping power of hydrogen ions between 30 and 140 keV in several metallic targets including Cu and Ni.

For energies below 30 keV, recent measurements of Morton *et al.*,⁹ Morita *et al.*,¹⁰ and Arkhipov and Gott¹¹ are in very poor agreement with each other, the differences being as large as 100%.

The present measurements cover the energy range between 25 and 250 keV, in which range experimental data are nonexistent or inconsistent. They also allow a comparison to be made with the above-mentioned low-energy data.

According to the theories of Lindhard and Scharff¹² and Firsov,¹³ the electronic energy loss for proton energies below 25 keV is expected to be proportional to the ion velocity v . Both theories use the Thomas-Fermi model for the projectiles and stopping atoms; therefore, no effects due to electronic structure are considered. The electronic stopping power thus calculated is given by a monotonously increasing function of z_1 , the atomic number of the projectiles, and of z_2 , the atomic number of the target atoms.

Recently, increasing attention has been paid to a periodic structure in electronic stopping power given as a function of z_1 , in a given stopping material, which is attributed to periodic fluctuations in the densities of electronic shells. This shell dependence has been first observed in amorphous and polycrystalline targets.¹⁴ The effect becomes more pronounced in electronic stopping through channels in single crystals.¹⁵ Theoretical treatments of the periodic structure as a function of z_1 , introducing Hartree-Fock electronic wave functions in the theories of Firsov¹³ and of Lindhard and Scharff¹² have been undertaken.¹⁶

The dependence of electronic stopping on z_2 for a given projectile has been first observed by Green *et al.*¹⁷ for protons of 500 keV. With protons of this same energy, Bader *et al.*⁵ observe a decrease of the stopping power in the region $23 \leq z_2 \leq 29$.

A similar decrease was also observed by Chu and Powers¹⁸ for He beams at energies between 0.8 and 2 MeV, and by White and Mueller⁸ for H and He beams at 100 keV. The latter authors comparing their data with that given by Hvelplund and Fastrup¹⁴ and considering targets up to $z_2 = 36$, point out a similarity between the z_2 and z_1 periodicity in that the maxima and minima appear at about the same positions.

The present measurements cover energies be-

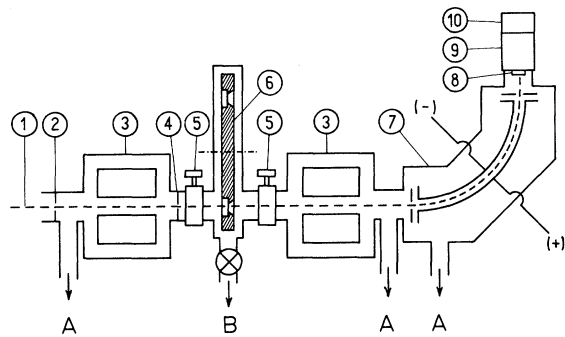


FIG. 1. Experimental arrangement. 1, proton beam; 2, beam monitor; 3, liquid-N₂ traps; 4, Adjustable two-slit assembly; 5, gate valves; 6, rotatable target holder; 7, electrostatic analyzer; 8, CsI crystal; 9, photomultiplier; 10, preamplifier. A, to liquid-N₂ trap and diffusion pump; B, to liquid-N₂ trap and mechanical pump.

tween 250 and 25 keV and are performed with target elements which are widely distributed through the Periodic Table. Therefore, they contribute to the information available for discussion of the dependence of the electronic stopping on the atomic number of the target.

II. EXPERIMENTAL METHOD

In the present work, the most direct method for obtaining the stopping power (dE/dx) has been used, namely, that of measuring the energy loss ΔE for a proton beam as it traverses a thin metal film of thickness Δx . For the results to be reliable, ΔE should be only a small fraction of the energy E of the incoming beam. At low energies and for solid targets, this method has the difficulty of requiring extremely thin self-supporting foils to fulfill the condition $\Delta E/E \ll 1$. For example, in order to have $\Delta E/E \leq 0.1$ for a 25-keV proton beam, the films must be less than 200 Å thick. Foils this thin were fabricated specifically for this purpose.¹⁹

Foil thicknesses were determined by first measuring the energy loss ΔE at 250 keV and using the stopping-power data given by Whaling^{1,2} at this energy.

This is equivalent to fitting the high-energy end of the present measurements to Whaling's curves.

Figure 1 gives a diagram of the experimental arrangement. The beam from the rf ion source of the Bariloche 350-keV Cockcroft-Walton accelerator is deflected through a 90° magnetic analyzer which holds the proton energy monoenergetic to within 0.1%. The beam traverses a liquid-N₂ cold trap and enters the target chamber. The targets are mounted on a manually rotating disc which can hold up to ten target foils.

After traversing a second liquid-N₂ trap, the beam enters a 90° 15-cm-radius electrostatic analy-

zer capable of resolving the proton energy within one part in 10⁴. The beam is finally detected by means of a scintillation counter consisting of a CsI crystal and a RCA 6342A photomultiplier.

The proton beam is defined by an adjustable two-slit assembly, located in front of the target chamber which limits the beam diameter to approximately 0.2 mm. The entrance and exit slits of the electrostatic analyzer have an aperture of 1 mm each.

In order to avoid damage of the thin target foils the beam currents used throughout this experiment were of the order of 10⁻¹⁴-10⁻¹⁵ A.

Three cold-trapped 2-in. diffusion pumps maintain a vacuum of the order of 2×10⁻⁶ Torr in the target and electrostatic analyzer chambers.

Rapid replacement of targets without disturbing the vacuum in the rest of the system is performed through a removable window, by first closing two gate valves located on either side of the target chamber.

Dry air is let in through a liquid-N₂ trap which also serves to avoid contamination by oil vapors when reevacuating.

Figure 2 gives a diagram of the electronics used to determine the energy losses of our proton beam. The electrostatic analyzer is polarized by means of two John Fluke model 410B 10-kV power supplies. The ground lead of the positive John Fluke supply is connected to an auxiliary power supply whose output is linearly and continuously changed from zero to its maximum voltage and vice versa

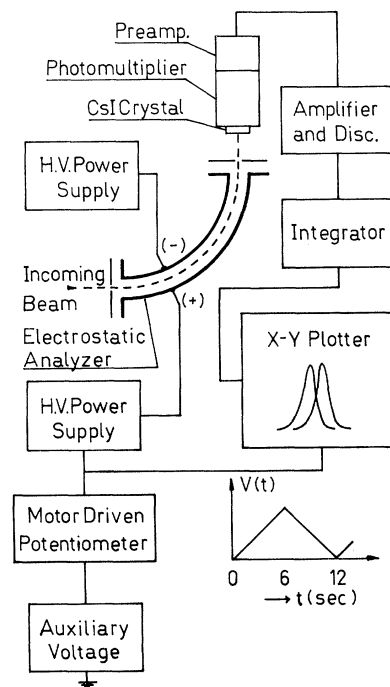


FIG. 2. Block diagram of the electronics used.

TABLE I. Typical relative energy losses $\Delta E/E$.

Target	Energy (keV)	
	200-250	25-40
Ni	2%	10%
Cu	6%	19%
Ag	3%	6%
Sn	2%	9%
Au	2%	10%

24 h of exposure to the atmosphere. No systematic change was observed in the measured energy losses.

(iii) By changing the target position with respect to the beam, the targets were found to be of uniform thickness within random errors. No pinholes were observed in the targets used.

(iv) Measurements for each metal were performed in targets of different thicknesses and the results normalized at 250 keV. The resulting stopping powers were in excellent agreement throughout the covered energy range, maximum discrepancies (at 25 keV) being less than 2%.

Random fluctuations of the measured energy losses for a given foil were less than 1%. Each stopping-power determination is calculated from measurements performed with at least two and, in certain cases, up to eight different foils for each metal. An individual measurement consists of taking ten energy spectra without, with, and without target, in that order.

Table I shows typical relative energy losses $\Delta E/E$ obtained in the present work. Except for copper all relative energy losses produced by our foils are 10% or less even at beam energies below 40 keV.

III. RESULTS AND DISCUSSION

In Fig. 4 our measurements are presented together with those corresponding to other authors.

a. Copper. After fitting the present data at 250 keV, the agreement obtained with Whaling's curve is excellent throughout the energy range of overlap. The curve corresponding to the review of Allison and Warshaw agrees well at the high-energy end but is 15% lower at 40 keV. The measurements of White and Mueller⁸ fall below our results. However, if fitted to our curve at one point, they would agree within 5% throughout the range of overlap. At very low energies we include measurements of Morita *et al.*¹⁰ and Arkhipov and Gott.¹¹ Whereas the results of Morita are somewhat higher than an extrapolation of our curve, their slope is clearly in agreement with ours. This is particularly significant because the slope of the stopping-power curves is expected to be constant and near $\frac{1}{2}$ at these low energies in a log-log representation. The slope of the curve of Arkhipov and

Gott, though constant, is neither $\frac{1}{2}$ nor in agreement with our data.

b. Silver. Fitting is performed with measurements of Porat and Ramavataram,⁷ which at higher energies are in agreement with Whaling.^{1,2} Our curve leads to an excellent fit in magnitude and slope to the stopping curve obtained by Morita *et al.*¹⁰ at very low energies.

c. Nickel. After fitting our curve to that of Whaling, the results of White and Mueller⁸ again lie below our results. We would like to point out that the slight indication of a maximum, as seen

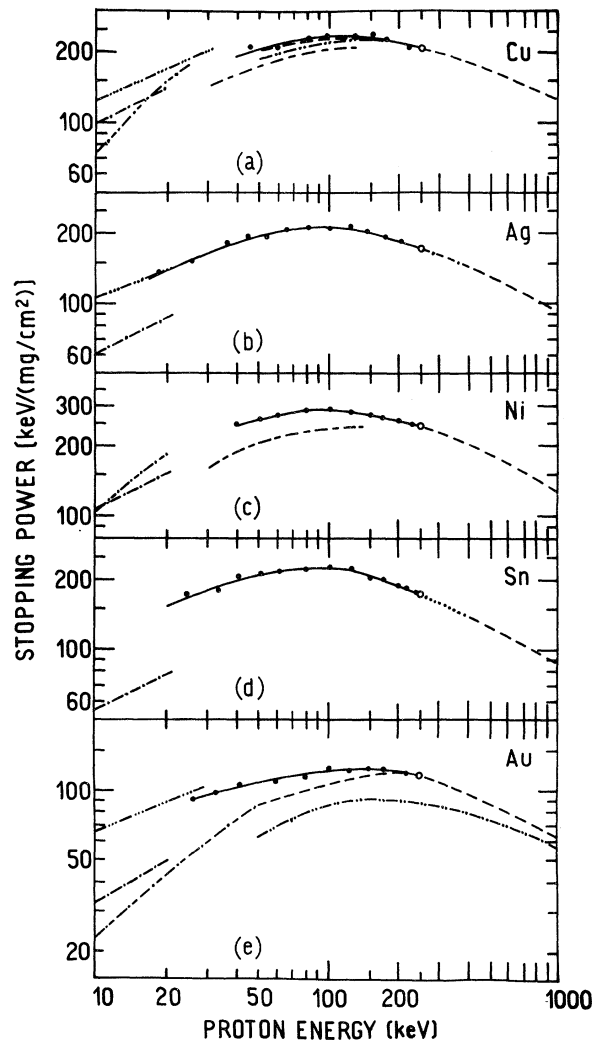


FIG. 4. Electronic stopping power for a hydrogen beam in Cu, Ag, Ni, Sn, and Au. (—) present work, probable errors fall within the dots; (---) Whaling, Refs. 1 and 2; (-·-·-·-) Allison and Warshaw, Ref. 6; (- - - - -) White and Mueller, Ref. 8; (-·-·-·-·) Morita *et al.*, Ref. 10; (-·-·-·-·) Arkhipov and Gott, Ref. 11; (-·-·-·-·) Porat and Ramavataram, Ref. 7; (-·-·-·-·) Morton *et al.*, Ref. 9; (-·-·-·-·) Lindhard and Scharff, Ref. 12; (···) extrapolation of Whaling's curve for Sn.

TABLE II. Stopping powers resulting from graphical interpolation of the experimental points in Fig. 4.

E_0 (keV)	$-\frac{dX}{dX}$ [keV/(mg/cm ²) ⁻¹]				
	Copper	Silver	Nickel	Tin	Gold
250	209	172	243	174	117
200	220	183	256	189	121
175	227	191	263	199	122
150	234	198	270	207	123
125	236	209	278	222	122
100	235	211	284	226	120
80	230	210	283	222	117
60	218	202	269	216	111
50	207	193	258	208	107
40	193	181	242	198	102
30		163		178	94
25		152		167	89
20		138		151	

in Whaling's curve between 200 and 300 keV, is not verified by our results. Our maximum stopping power is reached at 90 keV. There is an excellent fit in slope with Whaling's curve at higher energies. Once again, the slope of the curve of Arkhipov and Gott is not in agreement with an extrapolation of our data.

d. Tin. The low-energy limit of Whaling's curve for tin is 400 keV, corresponding to measurements of Green *et al.*¹⁷ Fitting of our data to their curve, extrapolated down to 250 keV, results in an excellent agreement of the corresponding slopes.

e. Gold. Whaling's curve extends down to 50 keV as in Cu. Fitting at 250 keV results again in a perfect fit in slope with the higher-energy data. However, our curve separates from that of Whaling, which at lower energies falls below ours. This leads to a shift in the energy at which the stopping power is maximum, from about 220 keV to approximately 140 keV. The data corresponding to the review of Allison and Warshaw fall up to 40% below our curve. At 30 keV our data fit within 4% of the low-energy measurements of Morita *et al.*¹⁰ A good agreement in slope is again observed with these authors. We also include measurements below 50 keV due to Morton *et al.*⁹ Their curve shows a strong difference in slope, leading to values for the stopping power of only $\frac{1}{3}$ of those of Morita at 10 keV.

In Table II we give the stopping powers which result from a graphical interpolation of our experimental points as given in Fig. 4.

In Fig. 4 we have also plotted the curves corresponding to the theory of Lindhard and Scharff¹² (slope 0.5) in its range of validity. As mentioned above, for the target elements common to the work of Morita and ours, there is good agreement in slope with the theoretical value. On the contrary,

the data of Arkhipov and Gott¹¹ and of Morton *et al.*⁹ lead to slopes approximately equal to 1, which would imply a v^2 dependence of stopping power. However, agreement in absolute value of the measured and theoretical stopping powers is not observed. The theoretical curves of Lindhard and Scharff¹² would, in all targets, fall below our extrapolated curves, as well as below the stopping powers measured by Morita *et al.*

Figure 5 shows the electronic stopping power per atom at energies of 200, 125, 50, and 25 keV as a function of z_2 , the atomic number of the target material.

The points with circles correspond to the present measurements. The rest of the information, including that for gaseous targets, is taken mainly from Whaling's¹ review data. At 200 keV, stopping powers corresponding to elements between $z = 20$ and 30 are due to Bader *et al.*⁵ At 125 and 50 keV those corresponding to $z = 24$ up to 29 are from White and Mueller,⁸ but shifted so that they agree with our data for Ni and Cu. Points are joined by full lines when they are not separated by more than two units in z_2 . Dotted lines are drawn if the separation is three or more units. These lines help to avoid confusion between points corresponding to different energies and represent only a rough indication of the z_2 dependence of the atomic stopping power. At 100 keV and for z_2 up to 35, a similar representation has already been shown by White and Mueller.⁸ Fluctuations are clearly observed. Their general shape seems to be rather independent of the beam energy.

We observe a first maximum at $z_2 \approx 7$ ($\frac{1}{2}\text{N}_2$) followed by a minimum at $z_2 \approx 10$ (Ne). A second maximum is located at about $z_2 \approx 23$ (V), as seen from the curve corresponding to 200 keV where data

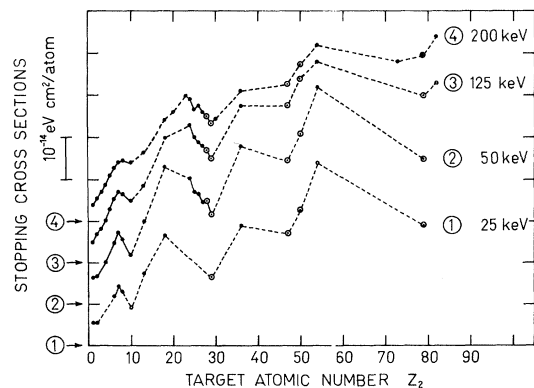


FIG. 5. Electronic stopping power vs z_2 (the atomic number of the target material) at energies of 200, 125, 50, and 25 keV. Arrows indicate the ordinate origin corresponding to the different curves. \circ : Data points from present work; \bullet : data points taken from previous works, see text for explanation.

of Bader *et al.*⁵ are available in the range $z_2 = 23$ – 29 . We find a minimum located at $z_2 = 29$ (Cu). The same position for the second maximum and subsequent minimum has been observed by Chu and Powers¹⁸ in the stopping of He beams at 800 keV and above, and is also indicated by the strong decrease in the stopping power for 100-keV He ions, measured by White and Mueller⁸ between $z_2 = 24$ and 29 . Although there are data for only two projectiles, this seems to indicate that the position of the maxima and minima as a function of z_2 is z_1 independent. This is analogous to the z_2 independence for the maxima and minima as a function of z_1 as pointed out by several authors. For $z_2 > 29$, fewer data are available. The stopping power seems to rise again as shown by the isolated point at $z_2 = 36$ (Kr), but nothing can be said as to the position of the maximum which is indicated by the 25- and 50-keV data. Our measurements may suggest the existence of a minimum between $z_2 = 36$ (Kr) and $z_2 = 47$ (Ag), followed by a subsequent rise through $z_2 = 50$ (Sn) and $z_2 = 54$ (Xe) when the $5p$ shell is

filled. From $z_2 = 54$ up to $z_2 = 79$ (Au) there is no information available, except for one point ($z_2 = 73$, Ta) at 200 keV. We can only suspect the existence of a minimum not far from $z_2 = 79$, followed by a subsequent rise through $z_2 = 82$ (Pb), which corresponds to the filling of the $6p$ shell.

Cheshire and Poate¹⁶ have theoretically calculated the z_1 dependence of electronic stopping through channels in single crystals, which have effectively one or a few impact parameters associated with the collision. In particular they discuss the case of stopping in the $\langle 110 \rangle$ channel of gold for $z_1 \leq 80$ and a beam velocity of 1.1×10^8 cm/sec. The theory of Firsov¹³ is used which, in calculating energy losses, considers the momentum transfer due to the passage of electrons out of the potential of one colliding atom to that of the other. Instead of determining the electron densities by the Thomas-Fermi model, Hartree-Fock-Slater orbitals are introduced. The resulting expression is symmetric with respect to projectile and target. The results of this calculation are shown in Fig. 2 of their

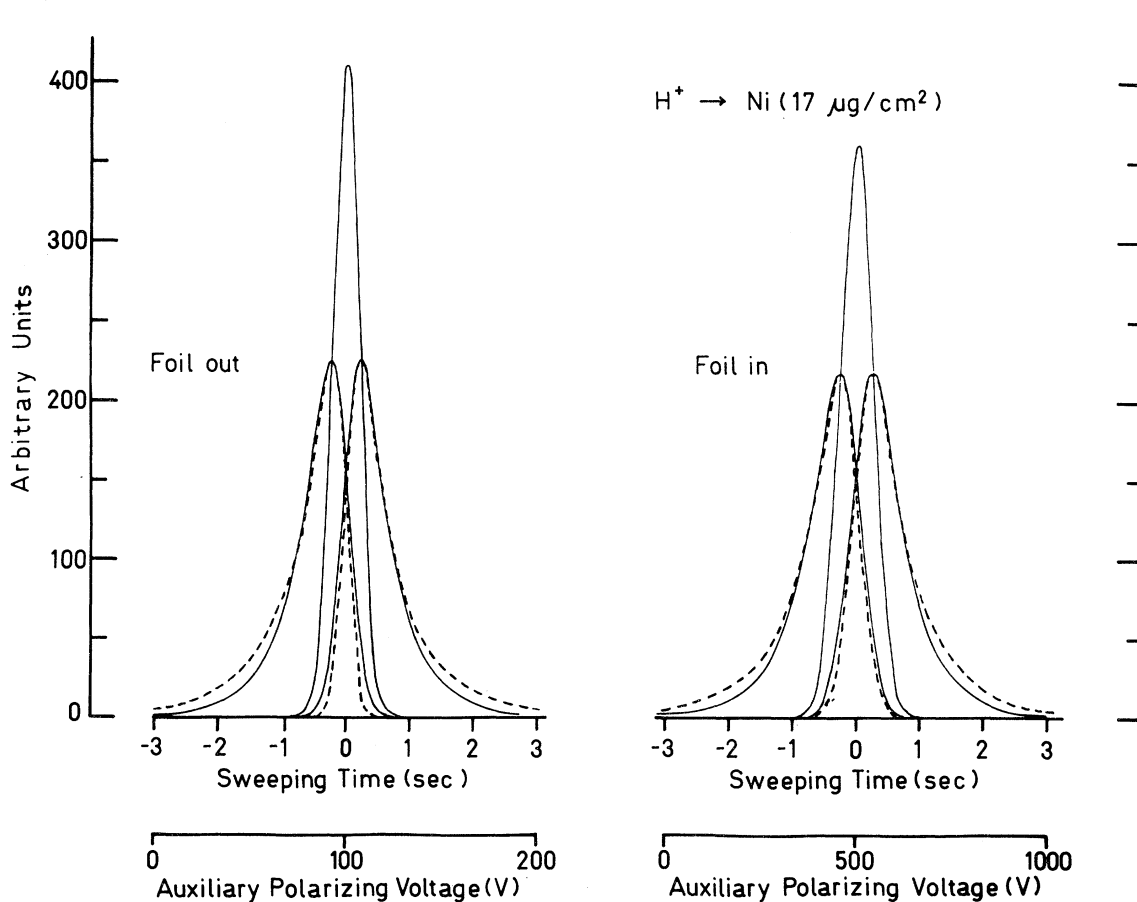


FIG. 6. Dotted lines: experimental response of dynamic recording system for a 63.4-keV incident hydrogen beam, and the same beam attenuated to 58.8 keV by a $17\text{-}\mu\text{g}/\text{cm}^2$ Ni foil. Full lines: corresponding Gaussian energy profiles and dynamic response computed according to Eq. (2).

paper. In spite of the fact that the theory deals directly with ion channeling in a specific case, up to $z_1 = z_2 \approx 35$, we observe a striking resemblance of the periodic structure shown by this theory, as compared to the experimental curves shown in Fig. 5. For higher- z values fewer experimental data are available and such resemblance is not obvious. (See note added in proof.)

Further study of the periodicity of the electronic stopping power as a function of z_2 at low beam energies is needed. The corresponding investigation is being carried out at present in this laboratory.

Note added in proof. Recently, C. C. Rousseau, W. K. Chu, and D. Powers [Phys. Rev. A **4**, 1066 (1971)] theoretically calculated stopping cross sections for 0.8–2.0 MeV α particles as a function of z_2 . The resulting periodicity, showing maxima at $z_2 = 6, 16, 20$, and 40, and minima at $z_2 = 10, 29$, and 46 is compatible with our Fig. 5 up to $z_2 = 54$ which represents the upper limit of their calculations.

APPENDIX

The differential equation governing the response of a dynamic recording system which has a time constant τ is given by

$$\tau \frac{du(t)}{dt} + u(t) = u_s(t). \quad (1)$$

This is the differential equation corresponding to a simple RC circuit.

By putting $\tau = 0$ it is seen that $u_s(t)$ represents the "static profile" one would get, not using a dynamic system, but rather measuring the spectrum point

by point.

If we assume for $u_s(t)$ a Gaussian shape $u_s(t) = Ae^{-\alpha t^2}$, then the solution to (1) is given by

$$u(t) = \frac{A}{2\tau} \left(\frac{\pi}{\alpha}\right)^{1/2} e^{1/4\alpha\tau^2} e^{-t/\tau} \left[1 + \operatorname{erf}\left(\alpha^{1/2}t - \frac{1}{2\alpha^{1/2}\tau}\right)\right], \quad (2)$$

where $\operatorname{erf}(x)$ represents the error function.

In Fig. 6 we have drawn the experimentally registered curves which correspond to an incident proton energy of 63.4 keV and a Ni foil of 17- $\mu\text{g}/\text{cm}^2$ thickness. The static distribution is represented by a Gaussian curve with $A = 410$, $\alpha = 11.1 \text{ sec}^{-2}$ for "foil out" and $A = 360$, $\alpha = 7.5 \text{ sec}^{-2}$ for "foil in." For convenience in computing, the Gaussian curve is centered at $t = 0$. The corresponding curves $u(t)$ are computed from (2) for the time constant $\tau = 0.5$ sec. It is seen that $u(t)$ turns out to be asymmetric and in principle very similar to our experimental curves. The curve for decreasing polarizing voltage is a mirror image of that for increasing polarizing voltage. This mirror symmetry, also observed in all the profiles measured in this work, is a proof of the symmetry of the corresponding static profiles.

The separation of the two computed peaks is equal to the separation of the peaks obtained experimentally. Our curves are not exactly reproduced by the computed $u(t)$, owing to the fact that the differential equation (1) is an oversimplification of the real experimental situation. For example, the inertia of the motor drive of the recorder has not been taken into account.

*Research sponsored in part by the Argentine Comisión Nacional de Investigaciones Espaciales, under Contract No. 17/68, and supported in part by the U. S. Air Force under Grant No. AFOSR-69-1802, monitored by the Air Force Office of Scientific Research of the Office of Aerospace Research.

†Captain Fuerza Aérea Argentina. Present address: Max-Planck Institut für Physik und Astrophysik, München, Garching, Germany.

‡Fellow of the Argentine Consejo Nacional de Investigaciones Científicas y Técnicas.

¹W. Whaling, *Handbuch der Physik*, Vol. XXXIV (Springer-Verlag, Berlin, 1958), p. 193.

²D. Demirlioglu and W. Whaling, California Institute of Technology, 1962 (unpublished).

³M. S. Livingston and H. A. Bethe, *Rev. Mod. Phys.* **9**, 245 (1937).

⁴F. Bloch, *Z. Physik* **81**, 363 (1933).

⁵M. Bader, R. E. Pixley, F. S. Mozer, and W. Whaling, *Phys. Rev.* **103**, 32 (1956).

⁶S. K. Allison and S. D. Warshaw, *Rev. Mod. Phys.* **25**, 779 (1953).

⁷D. I. Porat and K. Ramavataram, *Proc. Roy. Soc. (London)* **A252**, 394 (1959).

⁸W. White and R. M. Mueller, *Phys. Rev.* **187**, 499

(1969).

⁹A. H. Morton, D. A. Aldcroft, and M. F. Payne, *Phys. Rev.* **165**, 415 (1968).

¹⁰K. Morita, H. Akimune, and T. Suita, *J. Phys. Soc. Japan* **25**, 1525 (1968).

¹¹E. P. Arkhipov and Yu. V. Gott, *Zh. Eksperim. i Teor. Fiz.* **56**, 1146 (1969) [*Sov. Phys. JETP* **29**, 615 (1969)].

¹²J. Lindhard and M. Scharff, *Phys. Rev.* **124**, 128 (1961).

¹³O. B. Firsov, *Zh. Eksperim. i Teor. Fiz.* **36**, 1517 (1959) [*Sov. Phys. JETP* **9**, 1076 (1959)].

¹⁴J. H. Ormrod and H. E. Duckworth, *Can. J. Phys.* **41**, 1424 (1963); J. H. Ormrod, J. R. MacDonald, and H. E. Duckworth, *ibid.* **43**, 275 (1965); J. R. MacDonald, J. H. Ormrod, and H. E. Duckworth, *Z. Naturforsch.* **21a**, 130 (1966); B. Fastrup, P. Hvelplund, and C. A. Sautter, *Kgl. Danske Videnskab. Selskab, Mat.-Fys. Medd.* **35**, 10 (1966); P. Hvelplund and B. Fastrup, *Phys. Rev.* **165**, 408 (1968).

¹⁵L. Eriksson, J. A. Davies, and P. Jespersgaard, *Phys. Rev.* **161**, 219 (1967); F. H. Eisen, *Can. J. Phys.* **46**, 561 (1968); J. Böttiger and F. Bason, *Radiation Effects* **2**, 105 (1970).

¹⁶K. B. Winterbon, *Can. J. Phys.* **46**, 2429 (1968); C.

P. Bhalla and J. N. Bradford, *Phys. Letters* 27A, 318 (1968); I. M. Cheshire, G. Dearnaley, and J. M. Poate, *ibid.* 27A, 304 (1968); *Proc. Roy. Soc. (London)* A311, 47 (1969); I. M. Cheshire and J. M. Poate, *Atomic Collision Phenomena in Solids* (North-Holland, Amsterdam, 1970), p. 351.

¹⁷D. W. Green, J. W. Cooper, and J. C. Harris, *Phys. Rev.* 98, 466 (1955).

¹⁸W. K. Chu and D. Powers, *Phys. Rev.* 187, 478 (1969).

¹⁹A. Valenzuela and J. C. Eckardt, *Rev. Sci. Instr.* 42, 127 (1971).

²⁰J. B. Marion, *Rev. Mod. Phys.* 33, 139 (1961).